NASA/CR-2006-214509

CFD-Predicted Tile Heating Bump Factors Due to Tile Overlay Repairs

Victor R. Lessard
Genex Systems, LLC, Hampton, Virginia

September 2006

The NASA STI Program Office . . . in Profile

Since its founding, NASA has been dedicated to the advancement of aeronautics and space science. The NASA Scientific and Technical Information (STI) Program Office plays a key part in helping NASA maintain this important role.

The NASA STI Program Office is operated by Langley Research Center, the lead center for NASA's scientific and technical information. The NASA STI Program Office provides access to the NASA STI Database, the largest collection of aeronautical and space science STI in the world. The Program Office is also NASA's institutional mechanism for disseminating the results of its research and development activities. These results are published by NASA in the NASA STI Report Series, which includes the following report types:

- TECHNICAL PUBLICATION. Reports of completed research or a major significant phase of research that present the results of NASA programs and include extensive data or theoretical analysis. Includes compilations of significant scientific and technical data and information deemed to be of continuing reference value. NASA counterpart of peer-reviewed formal professional papers, but having less stringent limitations on manuscript length and extent of graphic presentations.

- TECHNICAL MEMORANDUM. Scientific and technical findings that are preliminary or of specialized interest, e.g., quick release reports, working papers, and bibliographies that contain minimal annotation. Does not contain extensive analysis.

- CONTRACTOR REPORT. Scientific and technical findings by NASA-sponsored contractors and grantees.

- CONFERENCE PUBLICATION. Collected papers from scientific and technical conferences, symposia, seminars, or other meetings sponsored or co-sponsored by NASA.

- SPECIAL PUBLICATION. Scientific, technical, or historical information from NASA programs, projects, and missions, often concerned with subjects having substantial public interest.

- TECHNICAL TRANSLATION. English-language translations of foreign scientific and technical material pertinent to NASA's mission.

Specialized services that complement the STI Program Office's diverse offerings include creating custom thesauri, building customized databases, organizing and publishing research results ... even providing videos.

For more information about the NASA STI Program Office, see the following:

- Access the NASA STI Program Home Page at ***http://www.sti.nasa.gov***

- E-mail your question via the Internet to help@sti.nasa.gov

- Fax your question to the NASA STI Help Desk at (301) 621-0134

- Phone the NASA STI Help Desk at (301) 621-0390

- Write to:
  NASA STI Help Desk
  NASA Center for AeroSpace Information
  7121 Standard Drive
  Hanover, MD 21076-1320

NASA/CR-2006-214509

CFD-Predicted Tile Heating Bump Factors Due to Tile Overlay Repairs

Victor R. Lessard
Genex Systems, LLC, Hampton, Virginia

National Aeronautics and
Space Administration

Langley Research Center
Hampton, Virginia 23681-2199

Prepared for Langley Research Center
under GSA Contract GS-00T-99-ALD-0209

September 2006

Available from:

NASA Center for AeroSpace Information (CASI)
7121 Standard Drive
Hanover, MD 21076-1320
(301) 621-0390

National Technical Information Service (NTIS)
5285 Port Royal Road
Springfield, VA 22161-2171
(703) 605-6000

SUMMARY

A Computational Fluid Dynamics investigation of the Orbiter's Tile Overlay Repair (TOR) is performed to assess the aeroheating Damage Assessment Team's (DAT) existing heating correlation method for protuberance interference heating on the surrounding thermal protection system. Aerothermodynamic heating analyses are performed for TORs at the design reference damage locations body points 1800 and 1075 for a Mach 17.9 and α=39° STS-107 flight trajectory point with laminar flow. Six different cases are considered. Interference heating results are presented for the TOR and the surrounding Thermal Protection System (TPS) tiles. The computed peak heating bump factors on the TOR surrounding tiles are below the DAT's heating bump factor values for the cases where the tiles are considered smooth. However, for uneven tile cases the peak interference heating is calculated to be considerably higher than the existing correlation prediction.

BACKGROUND

The Tile Overlay Repair (TOR) is an on-orbit patch for damage thermal protection tiles. Because the overlay protrudes out from the Orbiter outer mold line, the overlay alters the flow field and hence the heat transfer rates to the surrounding tiles. Short blunt protuberances, such as the TOR, can cause flow structures such as upstream separation or horseshoe vortices. These flow features can augment the local heating on the surface around the protruding object in high speed and hypersonic flow conditions. The amount of change in local heating is primarily dependent on the protuberance height (k), the boundary layer thickness (δ), and the boundary layer state. The distribution of heating in front of a protuberance is also dependent on the location and the number of vortices that develop. An experimental investigation done by Hung at Mach 5 wind tunnel conditions in 1980 and updated in 1984 provides an engineering correlation for estimating the interference heating on a flat plate in front of a protuberance [1,2]. Hung correlated the laminar flow heating in front of a blunt protuberance as a function of the ratio of the protuberance height to the boundary layer thickness (k/δ). The range of protuberance heights tested varied from $k = .6\,\delta$ to $k = 50\,\delta$. For short protuberances, such as the TOR, Hung's normalized heat transfer coefficient for laminar flow is given as

$$\max H_i/H_u = a \cdot (k/\delta)^{1.5}, \qquad 2.5 \leqq a \leqq 4.25 \qquad \text{Eqn. 1}$$

where max H_i is the maximum heating coefficient in front of the protuberance and H_u is the undisturbed heating coefficient without a protuberance [1, 2]. The present report refers to max H_i/H_u as the bump factor (BF). The orbiter entry aeroheating Damage Assessment Team (DAT) currently uses the upper bound of the coefficient range,

$$BF = 4.25 \cdot (k/\delta)^{1.5}, \qquad k/\delta \geqq 0.6 \qquad \text{Eqn. 2}$$

For protuberances where k/δ is less than 0.6, the DAT currently implements a linear fit

$$BF = 1.05 + 1.542 \cdot (k/\delta), \qquad k/\delta \leqq 0.6 \qquad \text{Eqn. 3}$$

Equations 2 and 3 are also referred to as the Boeing-Hung heating bump factor, because personnel of the Boeing Company are currently performing the DAT implementation. Note, equations 2 and 3 are equal when k/δ is 0.6. Cases considered in this report have k/δ values less than 0.6. Hence, comparisons are made between the computational fluid dynamics (CFD) predicted bump factors and the Equation 3 bump factor expression.

This report is divided into sections: the analysis method; the TOR cases analyzed; the results; and conclusions with recommendations.

ANALYSIS METHOD

Aerothermodynamic analysis of the TOR protuberance is performed using the Langley Aerothermodynamic Upwind Relaxation Algorithm (LAURA) code [3, 4]. LAURA is a three-dimensional, second-order finite volume flow solver for non-equilibrium chemistry. A five species chemical non-equilibrium, non-ionizing gas model (N, O, N_2, O_2, NO) for air is used. A radiation equilibrium wall temperature boundary condition is set at the surface. Reaction Cured Glass (RCG) catalycity and an emissivity of 0.89 are defined at the surface. A validation of the LAURA code for tile overlays has not been performed, being beyond the scope of the present work. The orbiter Configuration Control Board has accepted the LAURA code validation for baseline orbiter heat transfer and flowfield properties.

The freestream flow conditions correspond to a nominal Mach 18 point on the STS-107 trajectory [5]. The trajectory point angle-of-attack is 39.02°; the freestream velocity is 18164.33 ft/s; the density is 1.6294e-5 lb_m/ft^3; and the temperature is 429.21R. The flow is assumed laminar and steady. A comparison of the STS-107 trajectory, for which Mach 18 is the last point on the trajectory, to an International Space Station heavy vehicle forward weight (ISSHVFW) reference trajectory is shown in figure 1. The ISSHVFW trajectory is a fictitious trajectory, proposed for the Orbiter Return-To-Flight efforts, which represents the Orbiter's typical hypersonic entry conditions [6]. For comparison, the ISSHVFW trajectory includes a point with α=39.01°, V=18155.4 ft/s, T=435° R, and density 1.56×10^{-5} lbm/ft^3. The STS-107 point is used here to leverage existing orbiter CFD solutions, necessary for the time frame of the present study.

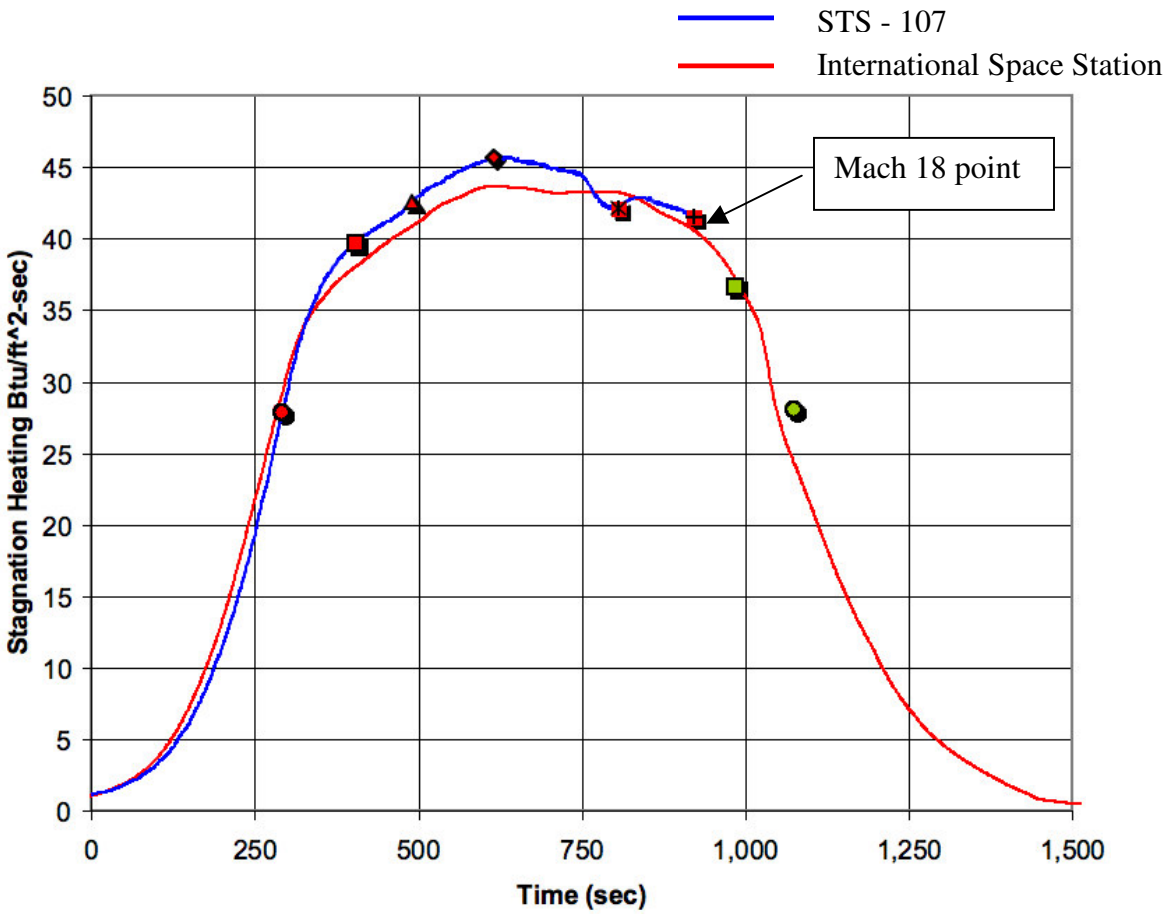

Figure 1 STS-107 and International Space Station trajectories.

Repair Modeling

To model the TOR on the full Orbiter using LAURA is beyond the scope of the present work. The problem is reduced by leveraging an existing LAURA solution for the Orbiter at the Mach 17.9 and α=39° trajectory point and using Langley's MORPH code. The MORPH code, developed by Gnoffo [7], was used in the grid generation and solution initialization of the TORs on the Orbiter. The software allowed the predefined TOR target shape to be used to generate a morphed grid with a protuberance at specified body point (Bpt) locations, 1800 and 1075 [8]. The TOR target definition had only to be oriented correctly based on the local surface normal and a rotation angle about the normal line. The morphing procedure operates on the specified grid blocks surrounding the TOR target location only. The morphed grid is blended with the surrounding nominal grid and the Orbiter solution is interpolated onto the morphed grid. The end result is a morphed

grid system that is a subset of the original Orbiter grid. A new flow solution is obtained only on this subset grid, on the assumption that the TOR only affects the local fluid domain. An example of the morphed grid system generated at the damage site Bpt 1800 is shown in figure 2. A MORPH journal file, which contains input data to the code, is included in Appendix A.

The TOR target shapes used in the MORPH code were generated as two-dimensional surface grids and projected conformally in the local normal direction onto the existing Orbiter grid outer model line (OML). This was assumed to give a good representation of the TOR molded onto the actual surface as long as the surface curvature was not too great. The MORPH code raises the TOR above the surface a given protruding distance. The TOR planform shape is a rectangle with dimension 25" x 15" with 2" corner radii. The top edge of the TOR is modeled as a sharp corner with zero radius. A simple rectangle TOR shape without the curved corners was modeled as a prototype case (Case 1) and also provides the parametric effects of the curved corners. The location of the center of the TOR at the Bpt 1800 site, based on the Orbiter's coordinate system, is x=1265", y=0", and z=261". The location of the center of the TOR at the Bpt 1075 site is x=330", y=45", z=301". Figure 3 shows the TORs on the Orbiter at the Bpt 1800 and 1075 damage locations. The TORs are modeled at a constant thickness – there is no modeling of the augers. The overlay and the gasket are modeled as a single unit, bumping out straight from the Orbiter surface. Two variables of overlay thickness are considered, 0.1 and 0.173 inches. This variation is intended to bound the upstream effects of the auger heights.

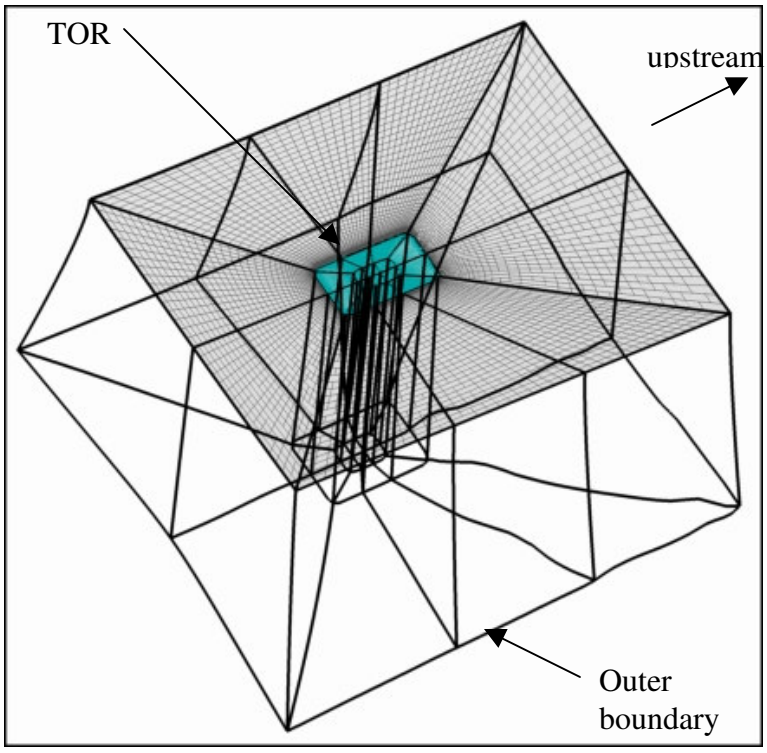

Figure 2 A TOR grid generated automatically by MORPH code. Surface grid and grid system blocking are shown.

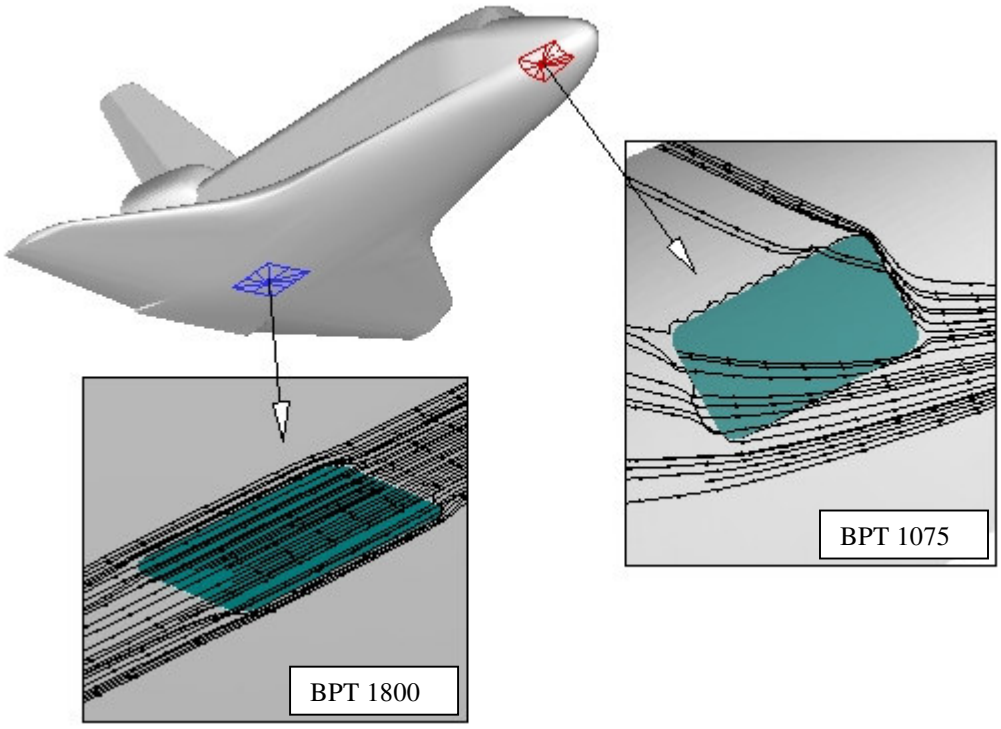

Figure 3 TOR locations BPT 1800 and 1075 on the Orbiter with flow direction depicted by streamlines.

Uneven Tiles Modeling

The Thermal Protection System (TPS) tiles on the Orbiter are designed with certain tolerances for the step heights between tiles because it is not possible to manufacture and place the tiles on the Orbiter with such accuracy that they are perfectly smooth. The allowable height tolerances, designated as MR by the Shuttle program, for forward and backward steps between neighboring tiles are +0.06 and –0.08 inches, respectively [8]. Thus, to realistically model the TOR on the Orbiter the "unevenness" of the tiles is considered. Variations of tile forward and backward step heights are referred to as "uneven tiles" in this report. To model the uneven tiles at the Bpt 1800 location the tile definitions for the Orbiter Atlantis is used. The tiles were given random heights that varied ±0.03" with the exceptions of several tiles at the forward face of the TOR (see figures 4 and 5). These tiles heights were manually set such that half of the front face height was 0.173 inches and the other half was 0.253 inches, a difference of 0.08", which is the MR allowable maximum step down. This was assumed to be a worst-case scenario. A "rough" tile case (Case 5) was initially generated where the front face heights were 0.173 inches and 0.391 inches. This case falls outside the allowable MR and

is ±0.14 inches. The case was generated prior to agreement on design specifications and is considered an extreme case that may not be realistic.

No gaps were modeled between tiles, nor is there a gap under the overlay. The tiles are not tilted, just stair stepped. Because a continuous computational grid is used, the steps between tiles are ramped over the computational cells at the tile edges, see figure 5 at the tile edges.

The roughness of the uneven tiles is inserted into the morphed grid blocks near the surface by projecting the grid onto the uneven tile database. The grid blocks at the surface were then redistributed in the normal direction based on the original grid normalized point distribution. Care was taken to maintain equal grid spacing between the surface blocks and the outer blocks above them.

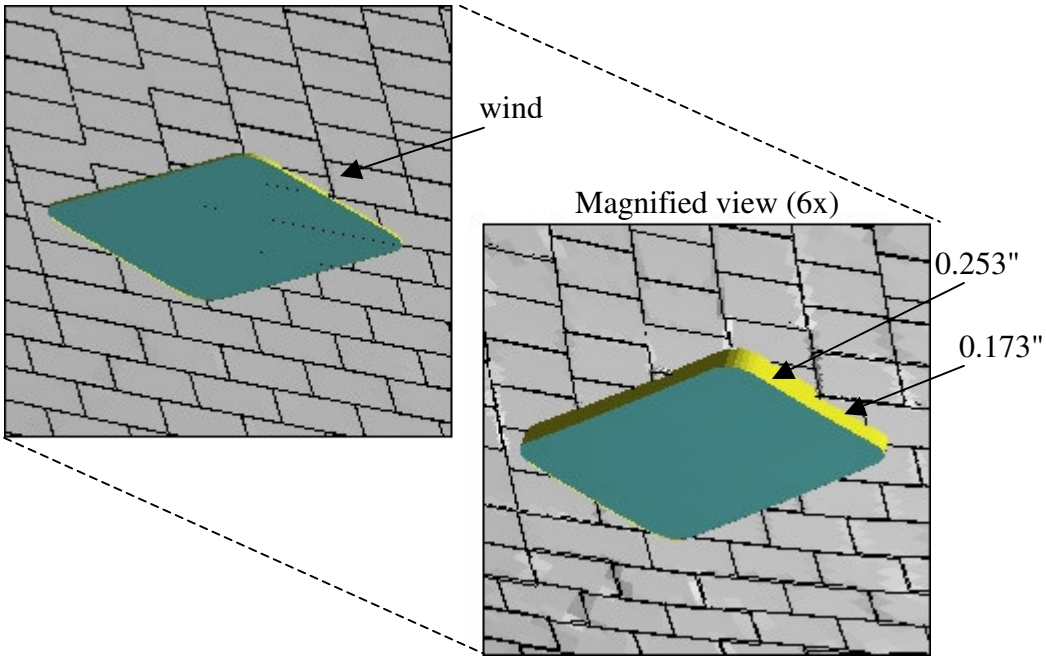

Figure 4 Modeling TOR placed on uneven tiles at the location Bpt 1800.

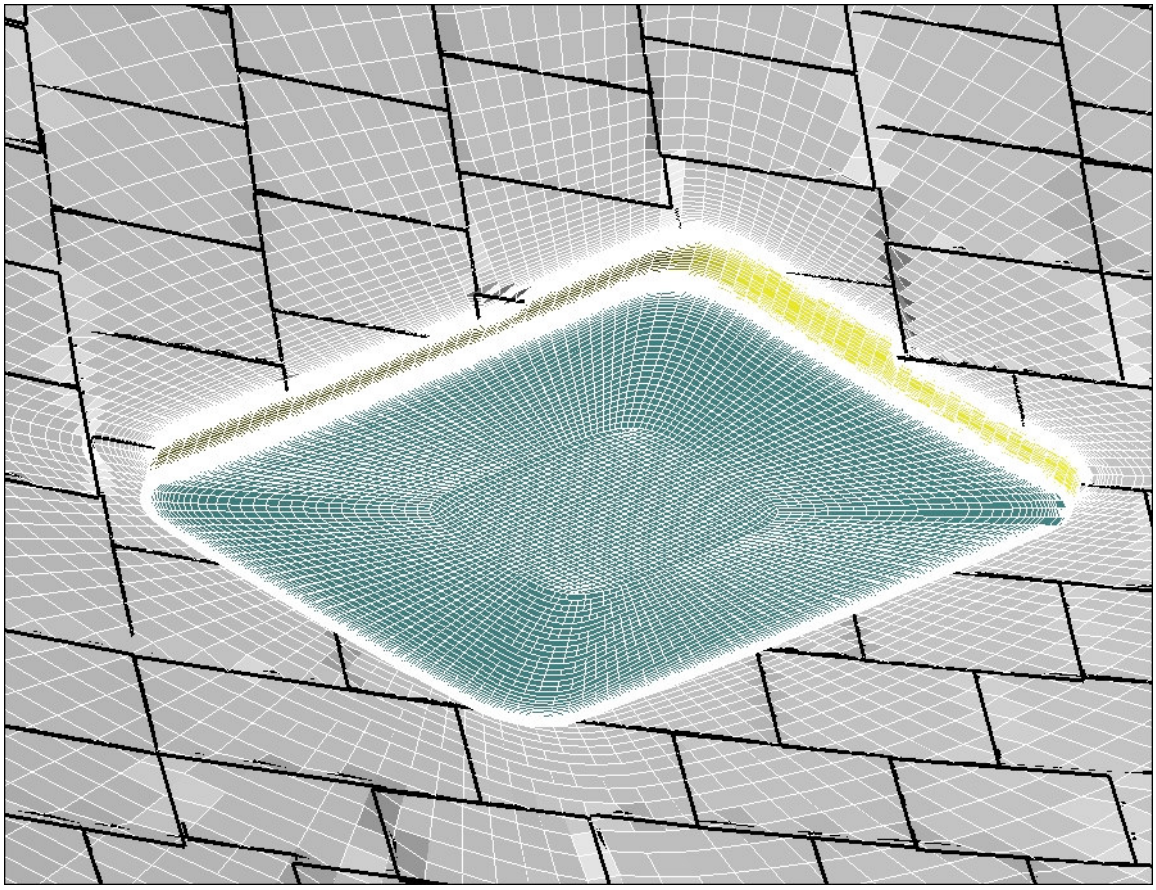

Figure 5 Grid modeling of TOR on uneven tiles at the location Bpt 1800. Vertical distance exaggerated 6x for visualization.

Morphed Grid Models

The grid models, generated by the MORPH code, for the six cases, discussed in the next session, can be grouped by their damage site location. The TOR grids at Bpt 1800 share the same grid topology and number of cells. These grids include the different TOR heights, the smooth and uneven tile cases, and the rectangle trial case. There are a total of 1.7 million cells in 36 grid blocks. Another 20 bounding blocks are used for exchange of boundary information, extracted from the full Orbiter solution. In the surface blocks surrounding the TOR the number of cells in the normal direction is 35. In the blocks above the TOR there are another 64 cells in the normal direction. Hence, there are a total of 99 cells across blocks from the tile surface to the outer boundary.

Similarly, the morphed TOR grid at Bpt 1075 location had a total of 1.8 million cells in 36 grid blocks. There are 24 bounding blocks used for exchange of boundary information, extracted from the full Orbiter solution. In the surface blocks surrounding the TOR the number of cells in the normal direction is 45. In the blocks above the TOR

there are another 64 cells in the normal direction. Hence, there are a total of 109 cells across blocks from the tile surface to the outer boundary.

Tile Overlay Repair Cases

The TOR cases analyzed are summarized in Table 1. The orientation positions 'flat-on' and 'corner-on' refer to the leading-edge location of the TOR based on the local flow direction. Case 1 at the body point 1800 is a trial case where the TOR is a rectangle with sharp corners. Case 1 also serves to determine the change in the predicted heating bump factor due to the rounded corners. The Boeing-Hung correlation does not differentiate heating effects due to variations in blunt protuberance shapes, only due to thickness variations. Cases 1 through 3, at Bpt 1800, are representative of TOR placement on smooth tiles with the gasket and overlay but not the augers as part of the thickness. The TOR thickness is 0.1 inches. The Case 3 TOR is rotated 30º such that one corner is the leading-edge, with respect to the local wind direction. This case is done to determine the orientation effect on the heating bump factor. Case 4 TOR, at Bpt 1075, is placed on smooth tiles of higher OML curvature with a thickness of 0.173 inches, which accounts for the thickness of the overlay, gasket and augers. The augers are not individually modeled. The repair has a constant thickness, which is expected to be an over-estimation of the auger contribution to the flow disturbances. This case verifies the heating bump factor for a higher k/δ parameter. The boundary layer is thinner, the TOR is thicker, and there is significant pressure gradient on the surface near the nose of the Orbiter.

Cases 5 and 6, at the Bpt 1800 location, are representative of TOR being placed on tiles that are uneven. The thickness of the TOR protuberance is 0.173 inches, the same as for Case 4. Both cases 5 and 6 frontal faces are split into two heights, assuming this is a worst-case scenario. Case 6 tile unevenness is according to the MR allowable of step-up height +0.06" and step-down height –0.08". Case 5 was undertaken prior to the consensus on the design specifications, and has doubled the unevenness of the tiles. This Case 5 is now considered an extreme case that is not necessarily realistic. The computational results of the six cases are presented in the next section of this report.

Case	Location	Height (k) inches	Orientation	Notes
1	1800	0.10	Flat - On	Full rectangle – no corner rounding
2	1800	0.10	Flat -On	
3	1800	0.10	Corner -On	
4	1075	0.173	Corner -On	Overlay plus auger height
5	1800	0.173 – 0.391	Flat - On	Very uneven (rough) tiles – (±0.14")
6	1800	0.173 – 0.253	Flat -ON	MR allowable uneven tiles – (+0.06", -0.08")

Table 1 TOR cases analyzed.

RESULTS

Results are divided into two parts: Part 1 focuses on surface heating and pressure on the tiles surrounding the TOR, and Part 2 focuses on surface heating on the top of the TOR with emphasis on the BPT 1800 cases 2, 3 and BPT 1075 Case 4. Part 2 results are compiled after the initial scope of the work was completed and is intended to provide heating bump factor data on top of the TOR.

The heating bump factors (BF) reported in Part 1 are referenced to an upstream value. The heating bump factors relative to the body point locations on the Orbiter can be determined by multiplying BF by a scale factor (γ) for the corresponding TOR case provided in table 2 below. The scale factor (γ) is the ratio of the TOR upstream local heating to the heating at the BPT location without TOR. In Part 2, the bump factors are referenced to the body point location, and are presented and designated BF_{bpt}.

$$BF_{bpt} = BF \cdot \gamma$$

Case	BPT Location	γ
1	1800	0.97
2	1800	0.97
3	1800	0.97
4	1075	1.11
5	1800	0.81
6	1800	0.89

Table 2 Scale Factor (γ) to compute the bump factor (BF) referenced to the body point (BPT) location.

Part 1

The LAURA results for TOR protuberance interference heating for the six cases are presented along with the DAT heating correlation results. Surface pressures are also provided along with the maximum differential pressures on the tile surface between the front and rear of the TOR. The differential pressure can be of use to assess the flow leakage under the TOR. Results are presented in form of line plots, color contours, and a table.

LAURA results for heating bump factor for all six cases are presented in figures 6 and 7. Figure 6 shows surface contours of the computed heating bump factor. Computed surface heat transfer rates are converted into bump factors by normalizing to a value of 1.0 approximately 10 inches upstream of the TOR. Data extraction lines, used for the line plots in figure 7, are depicted in figure 6 for reference. The extraction lines are designated as starboard, center and port. Starboard is a line extracted on the surrounding tile surface to the right (+y-direction) of the TOR. Center, as the word implies, is a line extracted down the center, excluding the TOR surface. Exclusion of the contours on the TOR surface is done to focus the reader's attention to the heating bump factors and pressures on the surrounding tiles. Inclusion of the TOR in the BF contours can be found in the Part 2 of the Results. The port line is extracted on the tile surface to the left (-y-direction) of the TOR. The data extraction line locations for the starboard and port varied slightly from the different cases due to positioning the lines at observed heating peaks. In figure 7 the computed heating bump factors are plotted versus the TOR x-direction location on the Orbiter. The Boeing-Hung heating bump factor is included in the line plots for comparison purposes.

Similarly, LAURA surface pressure results in the vicinity of the TORs are presented in figures 8 and 9. Figure 8 shows surface pressure contours of the tiles surrounding the TOR and figure 9 shows line plots of the extracted data lines. The same starboard, center and port data extraction lines are shown. The maximum pressure differential on the tile surface in front and behind the TOR is computed and the results are presented in Table 3. Table 3 summarizes the comparisons between the LAURA predictions and the Boeing-Hung correlations.

The CFD predicted heating bump factor for the surrounding tiles of the TOR is less than the Being-Hung correlation values for the body point 1800 cases 1, 2 and 3 where the $k/\delta=0.05$. The effect of interference heating due to the rounded corner Case 2 when compared to the trial Case 1 with sharp corners is minimal. The TOR for these two cases was aligned with the flow and is referred to in this report as being flat-on. The sharp corner Case 1 maximum heating bump factor was 1.0 compared with 1.1 for the Case 2 rounded corners. A small flow separation region occurred upstream of the front face. No increased heating was associated with it. The separation region flow feature was characteristic of all TOR protuberances analyzed in this report. The peak heating value occurs downstream past the trailing-edge corners. Vortices shed off the downstream corners cause increased heat transfer rates. For Case 3, where the TOR is rotated 30^o and the corner is the leading edge, the maximum heating bump factor of 1.0 was the same

as the sharp corner Case 1. There was little localized heating augmentation downstream of the corners.

The CFD-predicted maximum heating bump factor for the body point 1075 location Case 4, where $k/\delta=0.22$, was 1.0 compared to the Boeing-Hung correlation value of 1.38. The flow was aligned with the forward lower corner of the TOR. There was no significant heat transfer to the TOR surrounding tiles even though edge-shedding vortices developed and there is a pressure gradient across the protruding TOR.

For the last two cases, 5 and 6, the TOR, at Bpt 1800, is modeled on uneven height TPS tiles. The Case 5 tiles random heights are considered extreme and may not be representative of any actual tile placements on the Orbiter. The maximum k/δ for Case 5 is 0.19 and for Case 6 is .13. The surface tiles in front of the TOR were set at two different heights, which created asymmetric flow around the sides of the TOR. Vortices developed at both front corners and the corner with the greatest height developed a tighter, stronger vortex. A localized heat transfer rate hot spot developed beneath the stronger vortex. The heating bump factors at the upstream maximum height corner for Cases 5 and 6 were 2.8 and 2.1, respectively. It is uncertain whether it is the asymmetric flow around the TOR or the thickness of the TOR that pins the vortex to the corner, or the combination that creates the stronger vortex. Figure 10 shows the strong vortex at the corner, with a height 0.253 inches, for the uneven tile Case 6. The corner shedding vortices increased the heating on both sides of the TOR downstream. Higher heating occurs on the starboard side corresponding with the strong upstream corner vortex. Any tile on the side of the TOR that protruded up into the path of the strong vortex was a location where the heating bump factor jumped up. The rough tile Case 5 maximum heating bump factor was 3.9, which occurred on a protruding tile, with height $k=0.13$ inches, on the side of the TOR. For the Case 6 the maximum heating bump factor on the side of the TOR was 2.0.

Bpt 1800 – rectangle, k/δ=0.05

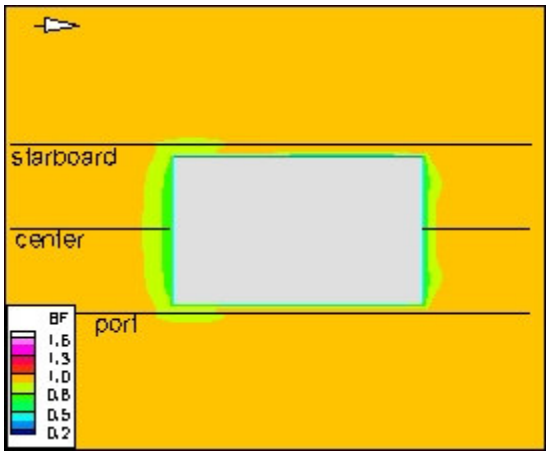

Bpt 1075 – k/δ=0.22

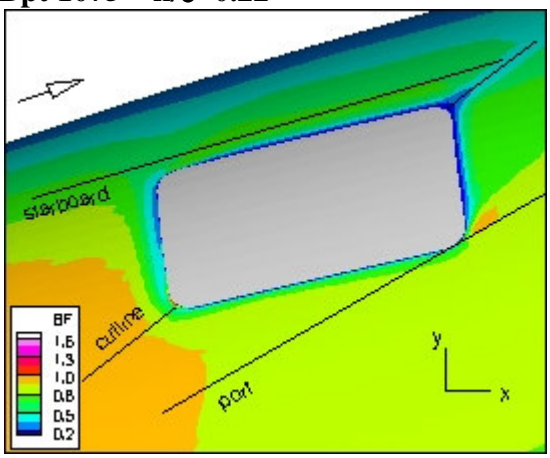

Bpt 1800 – flat-on, k/δ=0.05

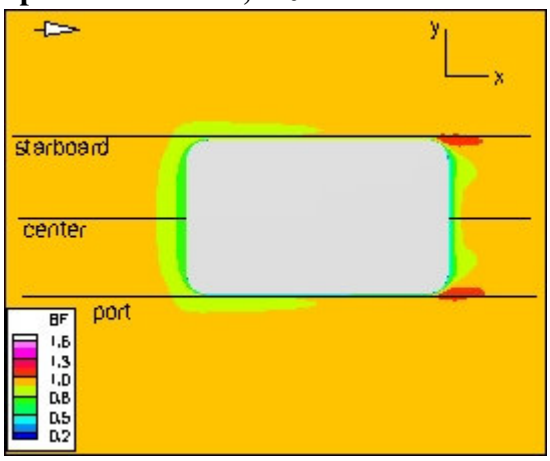

Bpt 1800 – rough tiles, k/δ=0.19

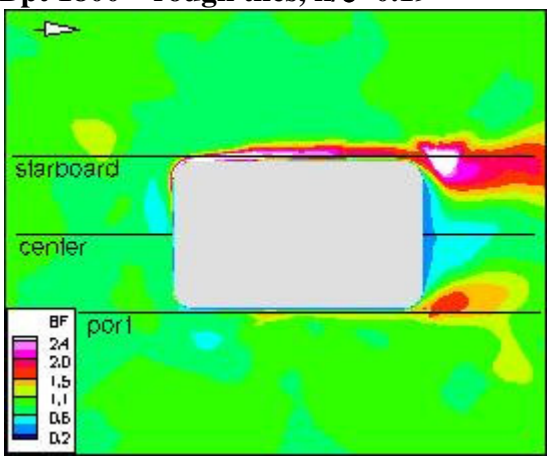

Bpt 1800 – corner-on, k/δ=0.05

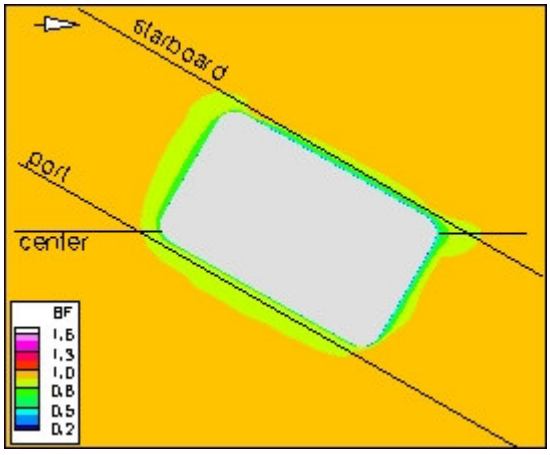

Bpt 1800 – uneven tiles, k/δ=0.13

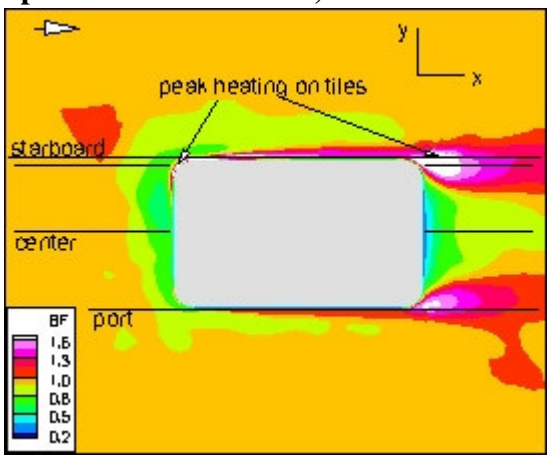

Figure 6 CFD predicted bump factor contours on tiles surrounding TOR.

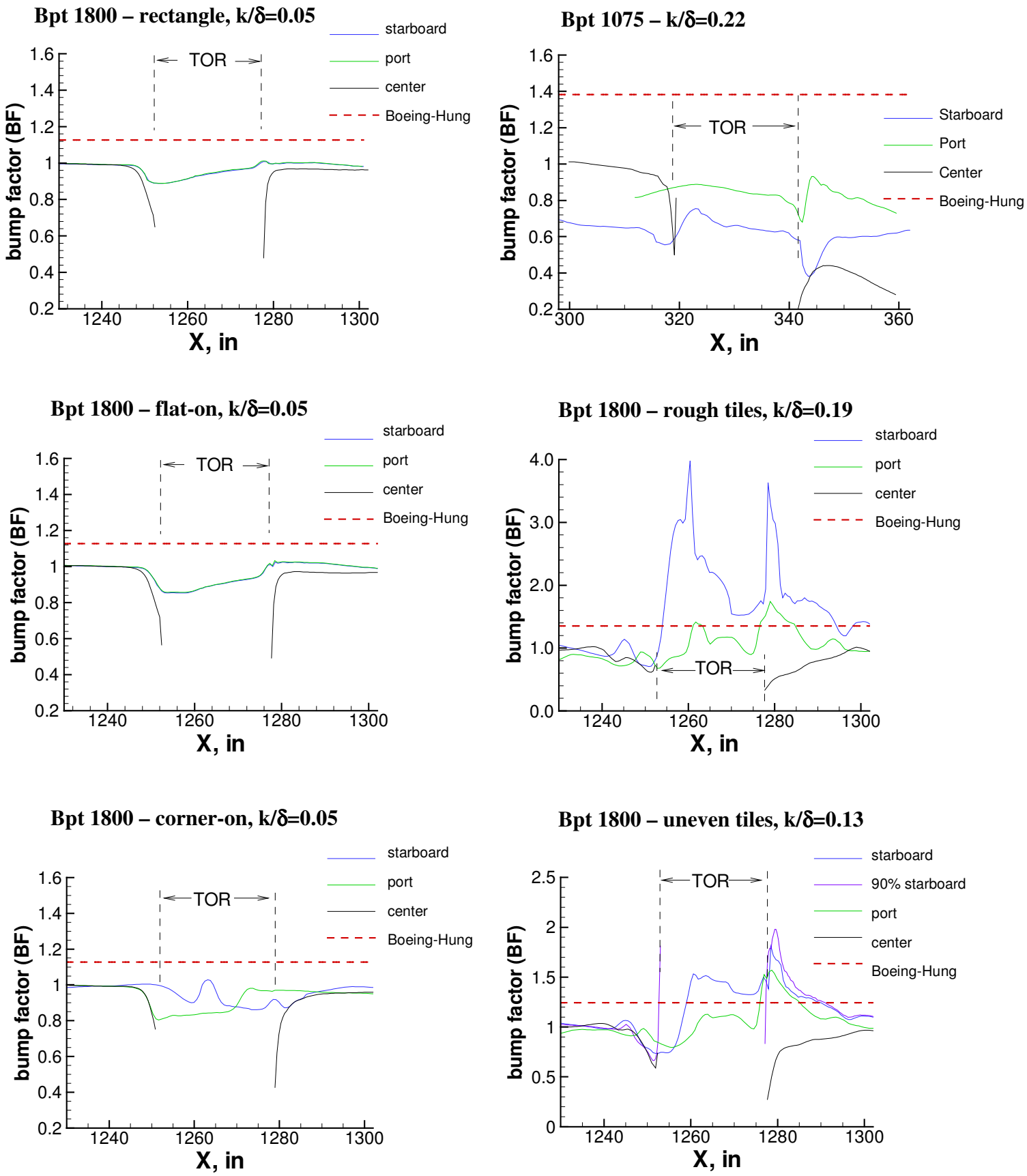

Figure 7 CFD predicted bump factors on tiles surrounding TOR.

Bpt 1800 – rectangle, k/δ=0.05

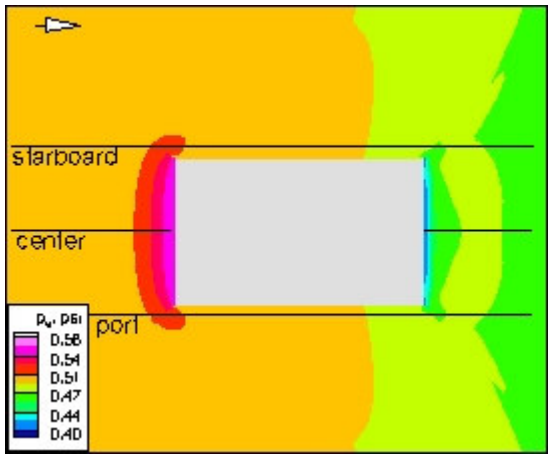

Bpt 1075 – k/δ=0.22

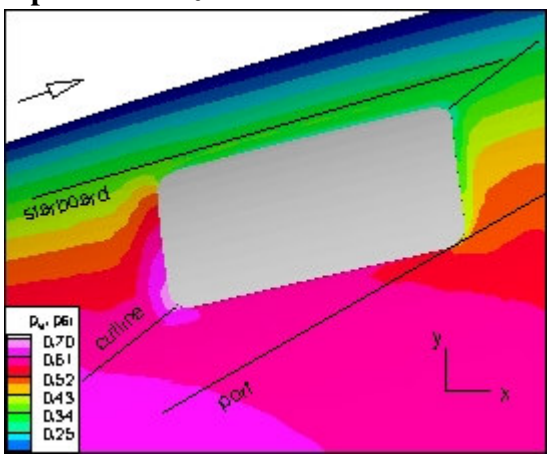

Bpt 1800 – flat-on, k/δ=0.05

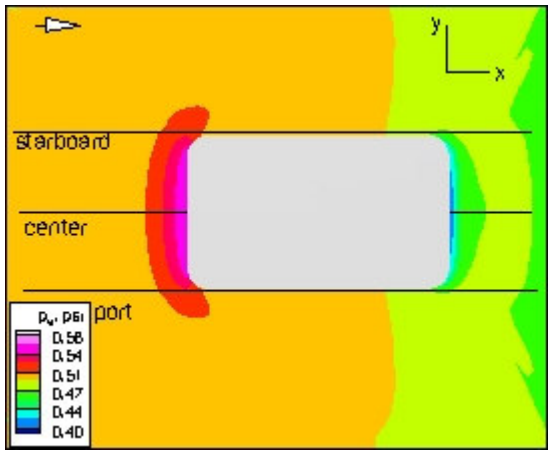

Bpt 1800 – rough tiles, k/δ=0.19

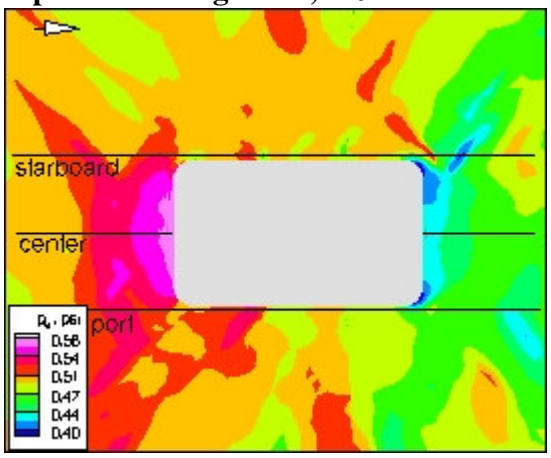

Bpt 1800 – corner-on, k/δ=0.05

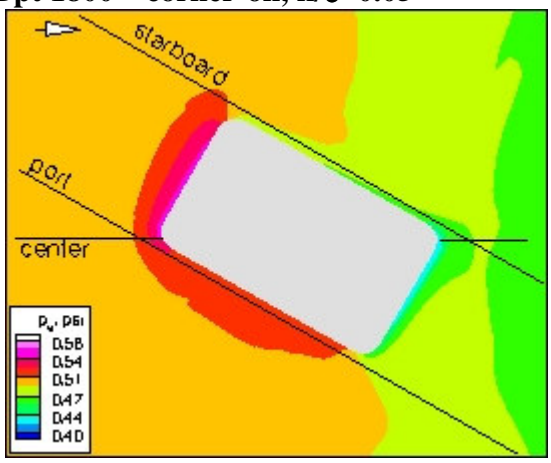

Bpt 1800 – uneven tiles, k/δ=0.13

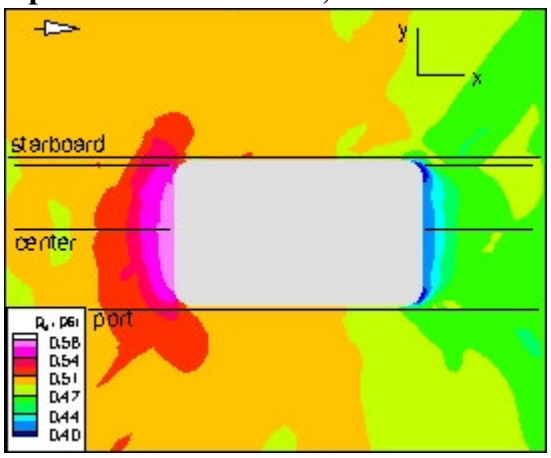

Figure 8 CFD predicted surface pressure contours on tiles surrounding TOR .

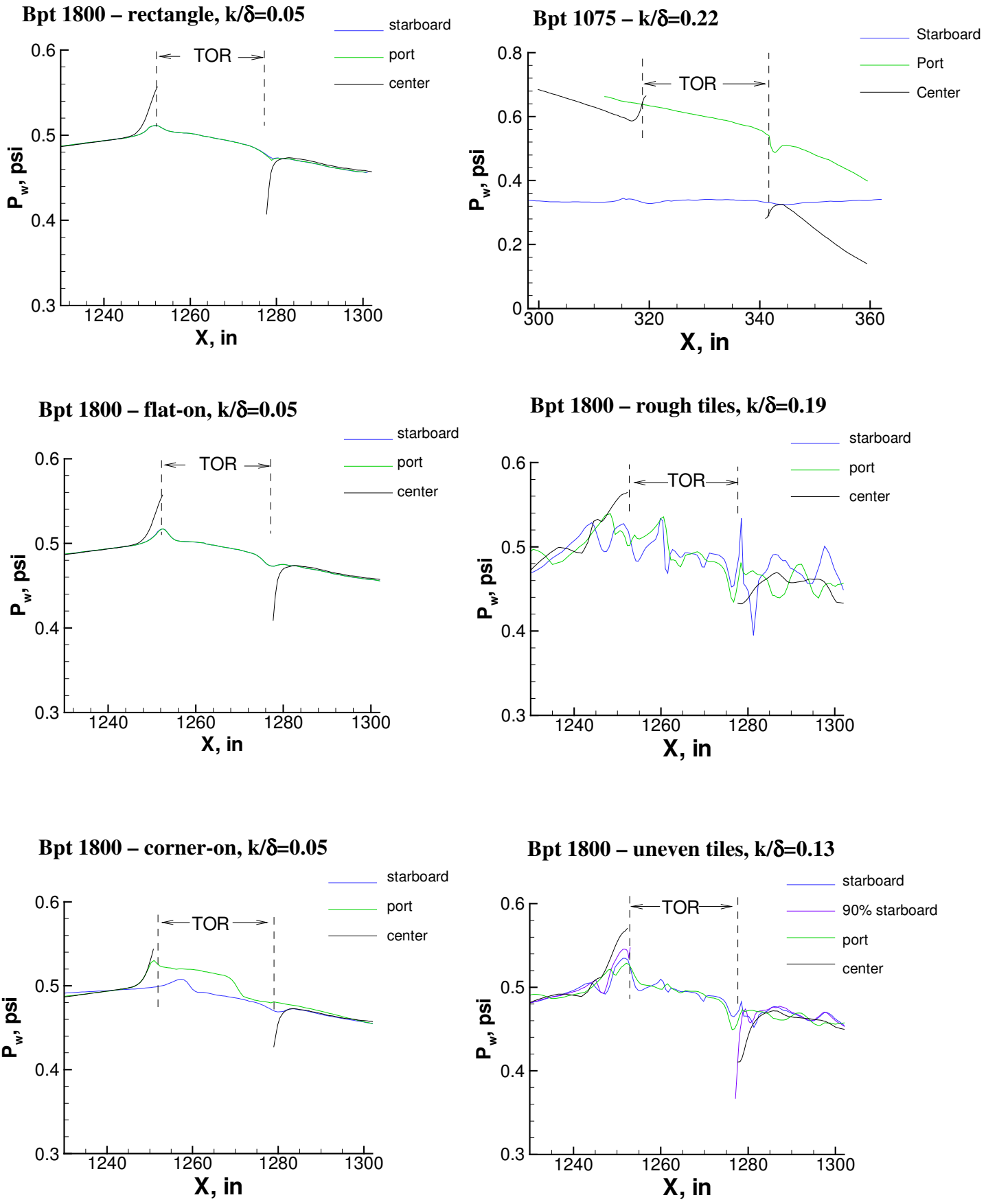

Figure 9 CFD predicted surface pressures on tiles surrounding TOR.

	Case	K (in)	δ (in)	K/δ	* Hung Upperbound BF	Computed BF	ΔP psi
1	BPT 1800 – rectangle	0.10	2.0	0.05	1.13	1.0	.15
2	BPT 1800 – flat-on	0.10	2.0	0.05	1.13	1.1	.15
3	BPT – corner-on	0.10	2.0	0.05	1.13	1.0	.11
4	BPT –1075	0.17	0.77	0.22	1.38	1.0	.39
5	BPT 1800 rough tiles	0.39	2.0	0.19	1.35	2.8 **, 3.9***	.14
6	BPT – uneven tiles	0.25	2.0	0.13	1.24	2.1 **	.15

* Boeing-Hung BF = 1.05 + 1.542(k/δ) for k/δ < 0.6
** peak heating upstream corner
*** peak heating on side protruding tile, not upstream

Table 3 Maximum upstream heating bump factors from LAURA computations.

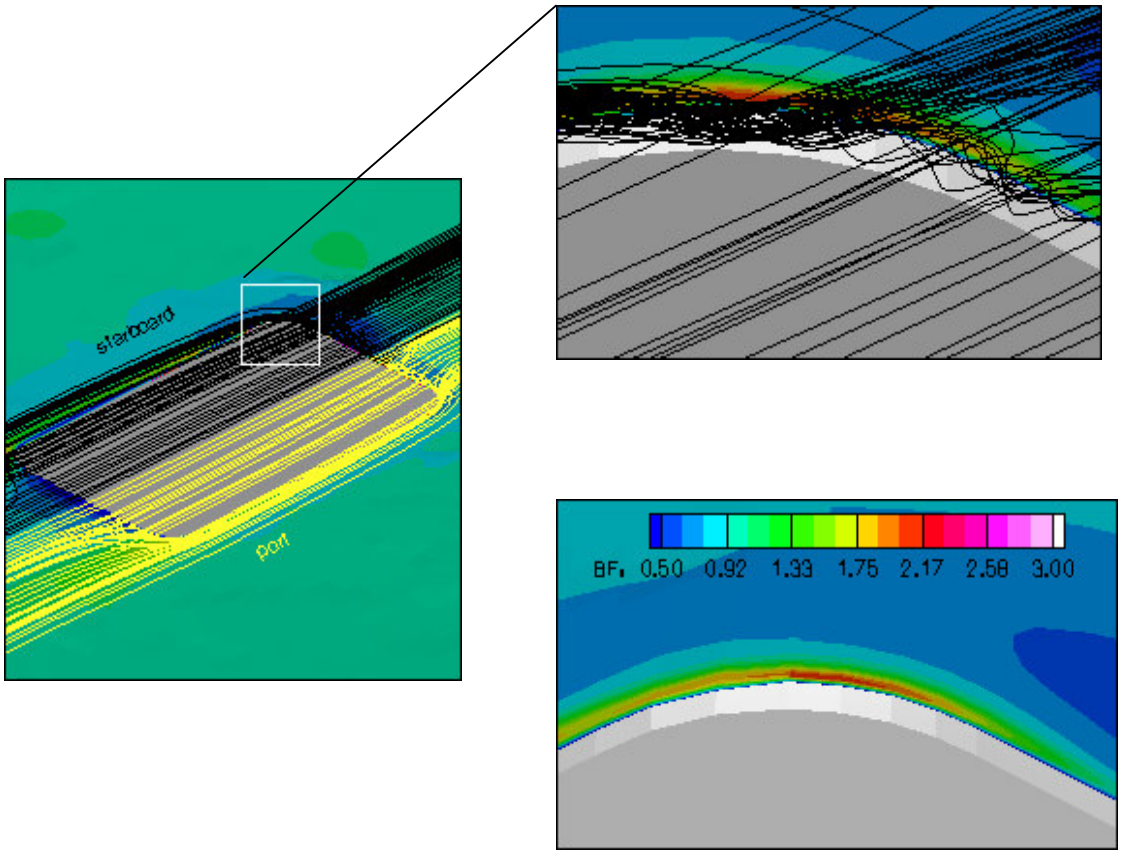

Figure 10 Vortex flow traces and heating bump factor contours near the front corner, of maximum height k=0.253'', for the uneven tiles case at Bpt 1800, Case 6.

Part 2

The computed heating rates for the top of the Tile Overlay Repair patch are reported in this section. The heating bump factors (BF_{bpt}), referenced to the body point location, are shown in figure 11 in the form of color contours for the six cases. The maximum heating occurs at the leading edge and around the corners of the TOR for all cases. Note that the edges of the overlay are modeled as sharp 90^o edges; the true overlay will have some small rounding of the edges, so that the computed peak edge heating is expected to over-predict the true heating. The heating rate for the majority of the area on the top of the TOR increased slightly above the nominal BF_{bpt} value of 1.0, excluding the edges. The heating increased at the downstream trailing edge of the TOR. More details of the heating bump factors for Cases 2 and 3 at body point 1800 and Case 4 at body point 1075 are provided in figures 12 through 15. In these figures, the heating bump factors are extracted along the local flow direction over the TOR. The distance along the extraction line is normalized by the total length across the TOR along the line and is designated as x/c. The extraction lines shown in the figures were considered to be representative of the heating bump factor over the entire TOR. Linear trend lines (or curve fits) that capture the essence of the BF distribution on the TOR were generated. The extreme peaks at the sharp leading edge were excluded in the determination of the trend lines. The sharp leading edge in the TOR computational model caused heating spikes at the edges due to the infinitely small radius and thus, it was considered unrealistic with respect to the actual TOR edges. The starting point of the trend lines was chosen near the end of the heating spike. Points that define the trend line are listed in the tables shown in the figures.

Figure 12 shows the heating bump factor results for the center and the port side on top of the TOR for the BPT 1800 Case 2. The starboard side is not shown because of the symmetry. The heating bump factor distribution is slightly higher toward the side edges of the TOR. A comparison of the BF_{bpt} trend lines between the "flat-on", port line extraction, case and the "corner-on" BPT 1800 case is shown in figure 14. The "flat-on" case bump factor distribution, along the port extraction line, is slightly higher than the "corner-on" case. Because of the similarity between the two cases a single trend line for the heating bump factor for the BPT 1800 cases for smooth tiles could be considered. The "flat-on" Case 2 heating bump factors trend line, on the port side, could be used to represent the heating bump factor distribution on a TOR protuberance where $k/\delta=0.05$ for different orientations, with respect to flow direction.

Figure 15 shows heating BF_{bpt} distribution from corner-to-corner along the flow direction and a distribution lengthwise of the TOR starting near the leading edge corner for Case 4. The two distribution trends are provided to help define a variation of the heating bump factor for the BPT 1075 case where $k/\delta=0.22$.

A summary of the mean bump factor values on the TOR for Cases 2, 3 and 4 of interest are provided in table 4. The mean bump factor values are computed as an area weighted arithmetic mean based on the computed heating rate over a surface cell area in the computational mesh. The computed mean heating bump factors on the top of the TOR for the BPT 1800 Cases 2 and 3 and the BPT 1075 case are less than the Boeing-Hung BF correlation.

Bpt 1800 – rectangle, k/δ=0.05

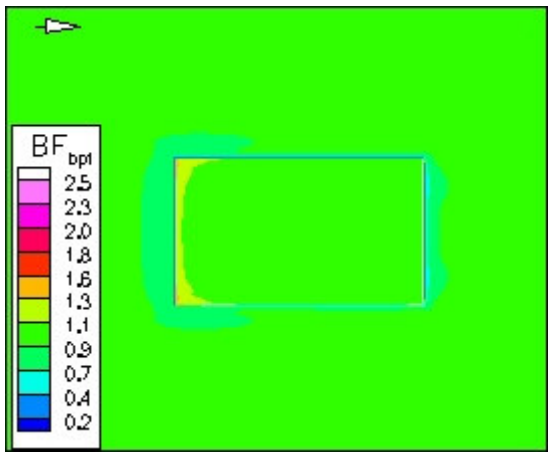

Bpt 1075 – k/δ=0.22

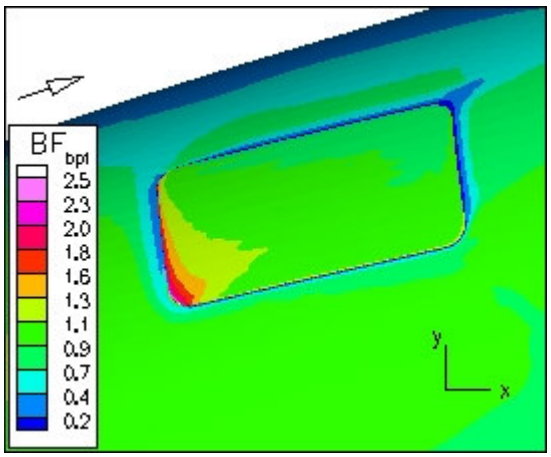

Bpt 1800 – flat-on, k/δ=0.05

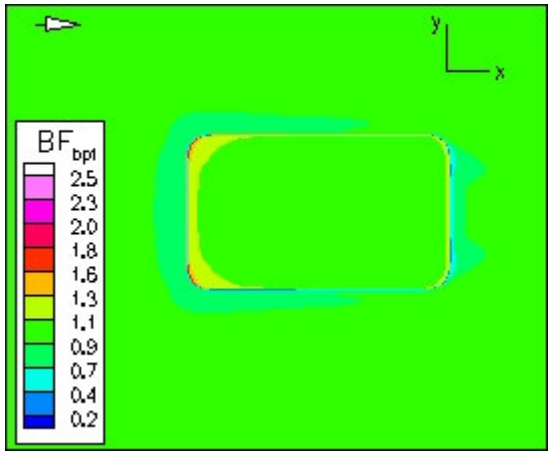

Bpt 1800 – rough tiles, k/δ=0.19

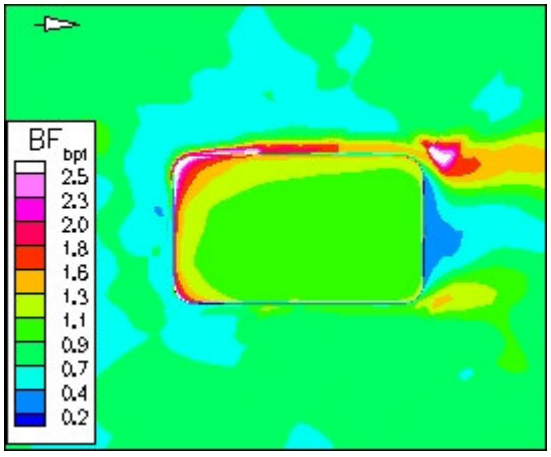

Bpt 1800 – corner-on, k/δ=0.05

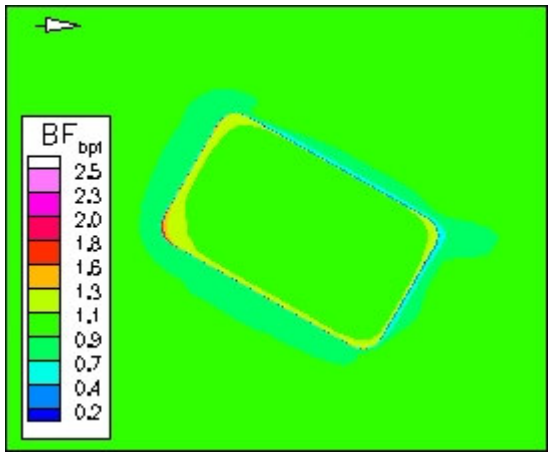

Bpt 1800 – uneven tiles, k/δ=0.13

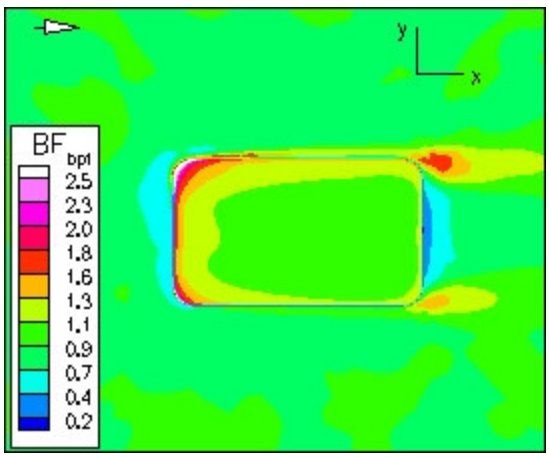

Figure 11 CFD predicted bump factor contours on TOR and surrounding TPS.

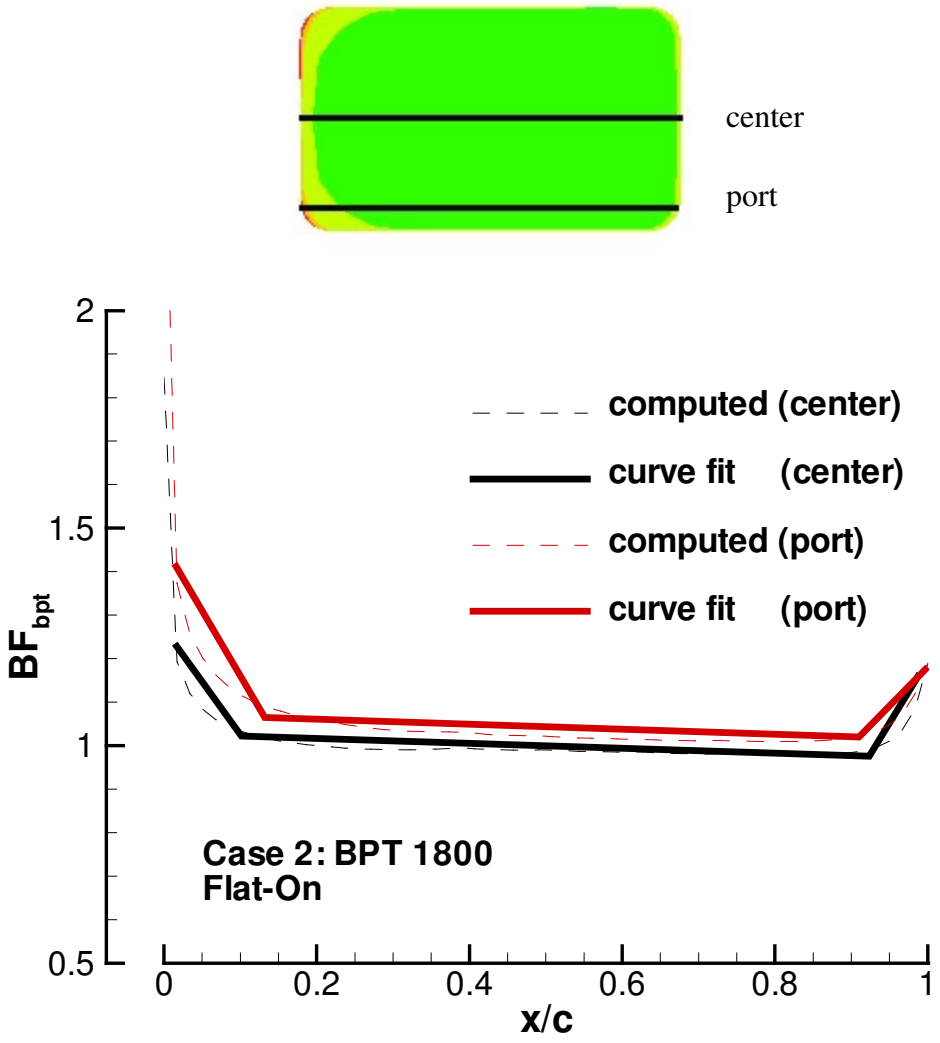

center

x/c	BF_{bpt}
0.017	1.23
0.10	1.02
0.92	0.98
0.99	1.16

port

x/c	BF_{bpt}
0.016	1.41
0.13	1.06
0.91	1.02
0.99	1.18

Trend Line Distributions

Figure 12 BF_{bpt} centerline distribution for BPT 1800 Case 2.

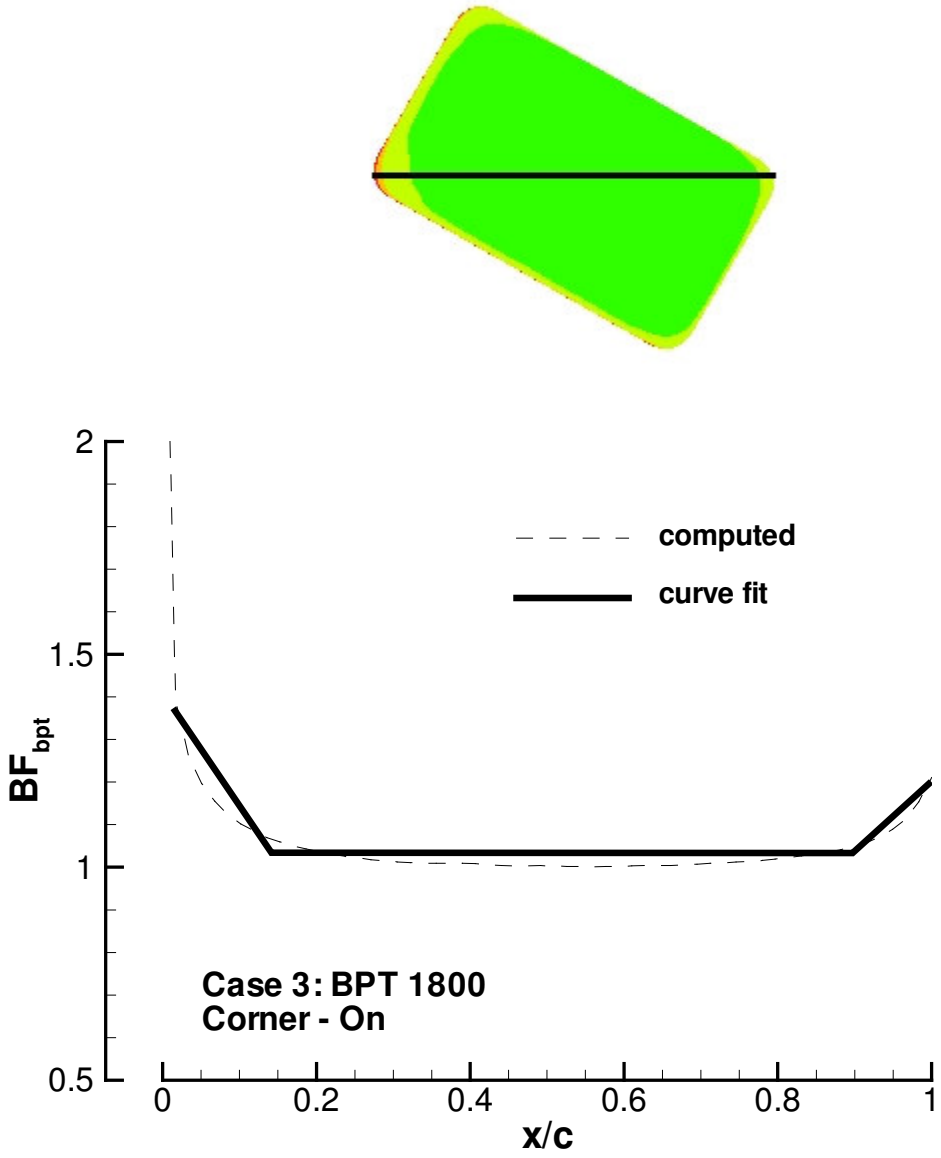

x/c	BF_{bpt}
0.016	1.37
0.14	1.03
0.90	1.03
1.00	1.20

Trend Line Distribution

Figure 13 BF_{bpt} corner-to-corner distribution for BPT 1800 Case 3.

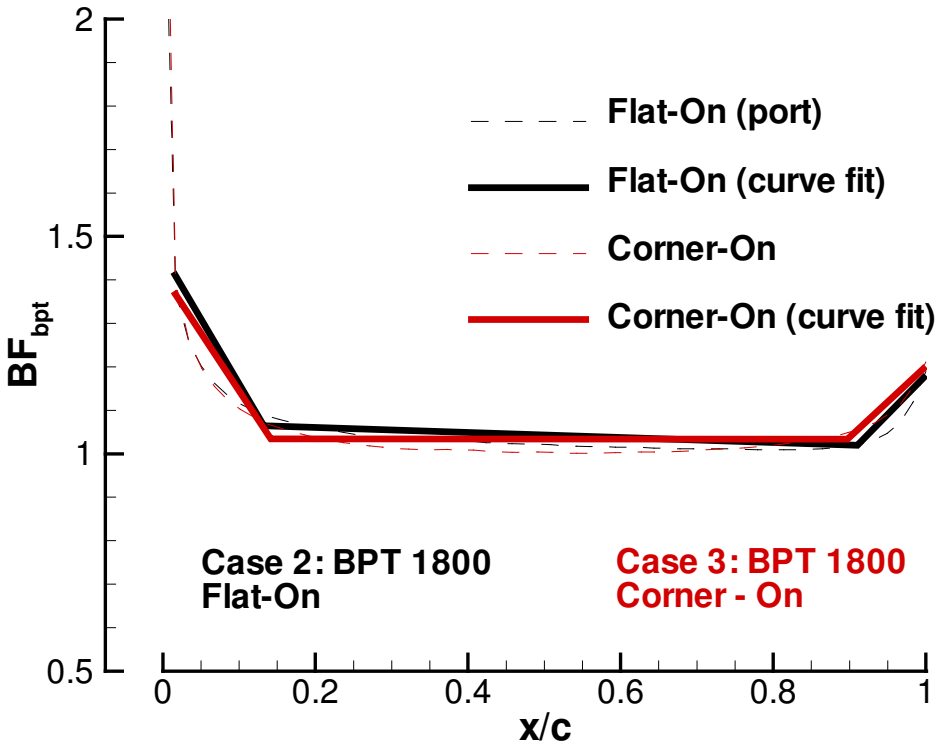

Figure 14 BF_{bpt} distribution comparison between BPT 1800 Cases 2 and 3.

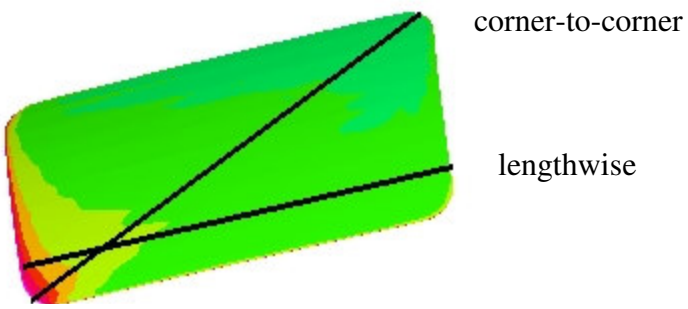

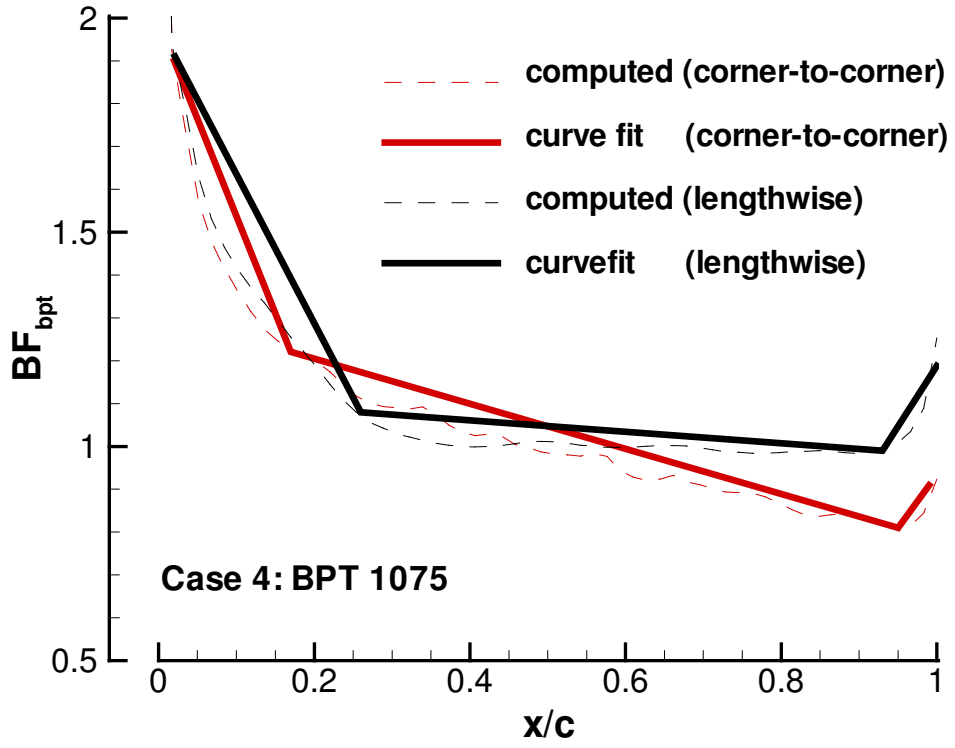

Corner-to-corner

x/c	BF_{bpt}
0.02	1.90
0.17	1.22
0.95	0.81
0.99	0.90

Lengthwise

x/c	BF_{bpt}
0.02	1.91
0.26	1.08
0.93	0.99
1.00	1.19

Trend Line Distributions

Figure 15 BF_{bpt} corner-to-corner and lengthwise distributions for BPT 1075 Case 4.

CASE	TOR mean BF_{bpt}	Hung Upperbound
(2) BPT 1800 – Flat-On	1.03	1.13
(3) BPT 1800 – Corner-On	1.04	1.13
(4) BPT 1075	1.00	1.38

Table 4 TOR mean heating bump factor comparison.

CONCLUSION

CFD predictions show that the computed peak interference heating bump factor (BF) on the tiles surrounding an overlay are below the Boeing-Hung BF values for the assumption of smooth tiles at both design reference site locations. The peak heating BF is considerably higher for both of the uneven tile cases 5 and 6, at the Bpt 1800 location. Specifically, the peak computed Case 6 BF is 2.1, versus 1.24 for the existing correlation prediction.

Asymmetric flow develops around the uneven front face of the TOR for the uneven tile cases. Vortical flow forms around the front curved corners. The front corner that has a higher forward facing step due to the uneven tiles heights has a stronger vortex. The combination of the asymmetric separated vortical flow and the strong corner vortex produces an upstream local surface-heating peak.

The stronger vortex flow down the side of the TOR causes increased surface heating on protruding tiles downstream as well as increased heating downstream of the aft corner where flow is turning again.

Simple trend lines for the heating bump factor distributions for the BPT 1800 and BPT 1075 Cases 2, 3 and 4 are developed. The CFD predictions for the mean heating bump factor on top of the Tile Overlay Repair for the BPT 1800 and BPT 1075 cases where smooth tiles are considered are less than the Being-Hung heating bump factor correlation.

RECOMMENDATIONS

For the uneven tile cases, where the tile steps are contrived in attempt to deliberately cause a worst case scenario, the peak heating hot spots cover a small portion of the exposed tile. A three-dimensional thermal analysis of the tile response to the computed heating distribution is recommended, to determine if these heating distributions would cause a safety of flight concern. Before the existing correlation is discredited, it needs to be determined if the high-resolution CFD results are resolving irrelevant details from the perspective of the thermal protection system performance.

If a thermal analysis does indicate that the CFD predicted heating distributions are a concern, then several follow-on steps should be taken. A validation of the LAURA code should be preformed for overlay geometries. An uneven tile CFD simulation should be performed with the overlay askew to the approaching flow, to see if the vortex confinement and hot spots still occur. The augers should be more accurately modeled for the uneven tile case, to see if the vortex confinement is inhibited with a smaller protuberance height. A more realistic modeling of the gasket should be performed such as ramping the overlay thickness instead of having a vertical leading edge. Another design reference location should be considered, on the centerline like body point 1800, but closer to the nose so that the boundary layer is thinner and the parameter k/δ is larger.

Acknowledgement

The author thanks William A. Wood of the NASA Langley Research Center Aero-Thermodynamics Branch for helpful recommendations and paper review.

REFERENCES

1. Hung, F.T. and Clauss, J.M., "Three-Dimensional Protuberance Interference Heating in High-Speed Flow," AIAA 18th Aerospace Sciences Meeting, AIAA-80-0289

2. Hung, F., and Patel, D., "Protuberance Interference Heating in High-Speed Flow," AIAA 19th Thermophysics Conference, AIAA-84-1724

3. Gnoffo, Pa. A., "An Upwind-Biased, point-Implicit relaxation strategies for viscous, hypersonic flows," AIAA Computational Fluid Dynamics Conference, 9th, June-13-15, 19189, AIAA-1989-1972

4. Cheatwood, F.M., and Gnoffo, P. A., "User's Manual for the Langley Aerothermodynamic Upwind Relaxation Algorithm (LAURA)," NASA TM 4674, April, 1996

5. Columbia Accident Investigation Board Report, Volume V, Appendix G.13, October 2003

6. Greene, F.A., and Hamilton, H.H., "Development of a Boundary Layer Properties Interpolation Tool in Support of Orbiter Return to Flight," 9th AIAA/ASME Joint Thermophysics and Heat Transfer Conference, AIAA 2006-2920

7. Gnoffo, P.A., "Grid Morphing Users Manual – Version 1.0," Feb. 13, 2006

8. Kinder, J., "Tile Overlay Repair Environments for Design Verification (status)," Damage Assessment Team Power Point slide presentation, March 1, 2006

APPENDIX A

The input file for the MORPH code used to generate the morphed grid from the full Orbiter's grid for the Bpt 1800 Case 2 is provided in this appendix for historical purposes in the event that additional work in the future is needed for TOR. Input files for the other cases are the same except for the grid blocks numbers and name of the target surface file.

Journal File of MORPH

```
          0  change default flags? 1=yes, 0=no
          1 solution format flag
point6.rst
          0  two-equation turbulence file flag
        438  number of blocks
          1  wall temperature file flag
point6.qtw
       -256  block number to be morphed
          5  OML surface index
          1  Morph all points on this surface?
          1  additional surfaces to be morphed?
        256  next block number to be morphed
          5  OML surface index
          1  Morph all points on this surface?
          1  additional surfaces to be morphed?
       -258  next block number to be morphed
          5  OML surface index
          1  Morph all points on this surface?
          1  additional surfaces to be morphed?
       -292  next block number to be morphed
          5  OML surface index
          1  Morph all points on this surface?
          1  additional surfaces to be morphed?
        258  next block number to be morphed
          5  OML surface index
          1  Morph all points on this surface?
          1  additional surfaces to be morphed?
        292  next block number to be morphed
          5  OML surface index
          1  Morph all points on this surface?
          0  additional surfaces to be morphed?
       -254  bounding block number
          5  OML surface index
          1  morph all points in block?
          1  additional bounding blocks to be morphed?
        254  next bounding block number
          5  OML surface index
          1  morph all points in block?
          1  additional bounding blocks to be morphed?
        255  next bounding block number
          5  OML surface index
          1  morph all points in block?
```

```
          1  additional bounding blocks to be morphed?
        257  next bounding block number
          5  OML surface index
          1  morph all points in block?
          1  additional bounding blocks to be morphed?
        291  next bounding block number
          5  OML surface index
          1  morph all points in block?
          1  additional bounding blocks to be morphed?
        294  next bounding block number
          5  OML surface index
          1  morph all points in block?
          1  additional bounding blocks to be morphed?
       -294  next bounding block number
          5  OML surface index
          1  morph all points in block?
          1  additional bounding blocks to be morphed?
       -291  next bounding block number
          5  OML surface index
          1  morph all points in block?
          1  additional bounding blocks to be morphed?
       -257  next bounding block number
          5  OML surface index
          1  morph all points in block?
          1  additional bounding blocks to be morphed?
       -255  next bounding block number
          5  OML surface index
          1  morph all points in block?
          0  additional bounding blocks to be morphed?
          0  damage outline index: -1 to n
bpt1800_patch_ascii.grd
          1  entries acceptable?
          0  0 to accept / 1 to override auto mapping
          0  reposition the damage center flag
 -1.000000      transition length for smoothing
          1  offset target surface flag: 0/1 = no/yes
 0.0800000      Offset distance. (total offset = .1 =.08+.02 target))
```

REPORT DOCUMENTATION PAGE

Form Approved
OMB No. 0704-0188

1. REPORT DATE *(DD-MM-YYYY)*	2. REPORT TYPE	3. DATES COVERED *(From - To)*
01- 09 - 2006	Contractor Report	

4. TITLE AND SUBTITLE

CFD-Predicted Tile Heating Bump Factors Due to Tile Overlay Repairs

5a. CONTRACT NUMBER

GS-00T-99-ALD-0209

5b. GRANT NUMBER

5c. PROGRAM ELEMENT NUMBER

6. AUTHOR(S)

Lessard, Victor R.

5d. PROJECT NUMBER

5e. TASK NUMBER

T03-01-S-L003

5f. WORK UNIT NUMBER

377816.06.03.03.08

7. PERFORMING ORGANIZATION NAME(S) AND ADDRESS(ES)

NASA Langley Research Center
Hampton, VA 23681-2199

8. PERFORMING ORGANIZATION REPORT NUMBER

9. SPONSORING/MONITORING AGENCY NAME(S) AND ADDRESS(ES)

National Aeronautics and Space Administration
Washington, DC 20546-0001

10. SPONSOR/MONITOR'S ACRONYM(S)

NASA

11. SPONSOR/MONITOR'S REPORT NUMBER(S)

NASA/CR-2006-214509

12. DISTRIBUTION/AVAILABILITY STATEMENT

Unclassified - Unlimited
Subject Category 34
Availability: NASA CASI (301) 621-0390

13. SUPPLEMENTARY NOTES

Langley Technical Monitor: William A. Wood
Preapred under GSA contract GS-00T-99-ALD-0209, Langley Task Order T03-01-S-L003
An electronic version can be found at http://ntrs.nasa.gov

14. ABSTRACT

A Computational Fluid Dynamics investigation of the Orbiter's Tile Overlay Repair (TOR) is performed to assess the aeroheating Damage Assessment Team's (DAT) existing heating correlation method for protuberance interference heating on the surrounding thermal protection system. Aerothermodynamic heating analyses are performed for TORs at the design reference damage locations body points 1800 and 1075 for a Mach 17.9 and a=39° STS-107 flight trajectory point with laminar flow. Six different cases are considered. The computed peak heating bump factor on the surrounding tiles are below the DAT's heating bump factor values for smooth tile cases. However, for the uneven tiles cases the peak interference heating is shown to be considerably higher than the existing correlation prediction.

15. SUBJECT TERMS

Orbiter; Aeroheating; Bump factor; Computational fluid dynamics; Protuberance; Thermal protection system; Tile overlay Repair

16. SECURITY CLASSIFICATION OF:			17. LIMITATION OF ABSTRACT	18. NUMBER OF PAGES	19a. NAME OF RESPONSIBLE PERSON
a. REPORT	b. ABSTRACT	c. THIS PAGE			STI Help Desk (email: help@sti.nasa.gov)
					19b. TELEPHONE NUMBER *(Include area code)*
U	U	U	UU	33	(301) 621-0390